

pubs.acs.org/crystal Article

Single-Component Globular Systems Capable of Plastic or Elastic Deformation and Structural Transitions

Sanjay Dutta and Caleb D. Martin*



Cite This: Cryst. Growth Des. 2023, 23, 8173-8180



ACCESS I

Metrics & More

Article Recommendations

Supporting Information

ABSTRACT: Elastic and plastic bending, as well as temperature-induced reversible and irreversible structural transformations, are revealed in single-molecule bicyclic phosphates. These bending properties are rare for globular systems. Structure—property analyses by single-crystal X-ray diffraction and calculations rationalize the observed behaviors. Collectively, this work identifies this class of molecules as promising candidates for flexible ferroelectric materials.



■ INTRODUCTION

Ordered molecular materials that retain crystalline properties under mechanical stress are important to develop flexible electronic materials.^{1–5} Applications in this realm include mechanical actuators, ⁶⁻⁸ molecular machinery, ^{9,10} flexible luminescent materials, ¹¹⁻¹³ optical waveguides, ¹⁴⁻¹⁸ and sensors. ¹⁹ Mechanosalient materials^{5,20} can change shape by bending, ^{21–32} twisting, ^{33–39} or coiling, ^{40,41} similar to polymers, liquid crystals, ⁴² and elastomers. ^{43,44} A material is considered flexible if it undergoes elastic or plastic deformation. 5,45 Crystalline materials are rigid structures that upon deformation typically fracture. However, plastic and elastic crystals are not susceptible to fracturing. Plastic crystals undergo permanent deformation upon application of an external mechanical force, whereas elastic crystals restore their original shape upon the removal of the external force. Reddy and co-workers defined plastic behavior in single crystals of organic molecules by the slip plane model.46 In this model, the slip planes are held together by weak dispersive interactions between the layers. The anisotropy in the intermolecular interaction strength makes the slip planes along different directions capable of bending. In contrast, the interactions in elastic crystals are energetically isotropic in orthogonal directions.

The majority of systems that exhibit bending properties (plastic and elastic) are molecules with flat geometries. ^{21,22,25} Desiraju's bending model of 2D + 1D anisotropic packing determined that crystals with a short crystallographic axis (known as 4 Å structures) are feasible candidates for plastic bending. ^{46,47} However, Thomas and co-workers showed plastic bending in dimethyl sulfone crystals that feature isotropic interactions, deviating from Desiraju's model. ²⁶ Mondal and

co-workers demonstrated 3D plastic bending in amino-borane Lewis acid-base adducts that also exhibit exceptional metallike ductility and malleability. 40 The exceptional plasticity is attributed to the multiple slip planes and weak electrostatic interactions around the molecular columns. Recently, Das and co-workers reported room-temperature elastic and plastic bending in metal oxyacid crystals of dimethylammonium perrhenate.47 At elevated temperatures, the malleability increased significantly, attributed to the crystal adopting a highly symmetric rotor phase. It is noteworthy that in the aforementioned studies, they are globular systems as either Lewis acid—base adducts or salts, 40,47 both highly polar. We hypothesize that bicyclic phosphates could be suitable candidates for mechanically flexible materials due to their globular geometry (globularity > 0.85 G, 0.12 Ω > asphericity) and polar nature.⁴⁸ In this work, we examine the elastic and plastic bending in bicyclic phosphate crystals that feature a methyl or ethyl tail and phosphine oxide or phosphine sulfide head (1-4, Figure 1).

■ RESULTS AND DISCUSSION

The bicyclic phosphates 1–4 were synthesized by the literature methods.^{49,50} Single crystals of 1 and 2 were obtained by sublimation, 3 were grown from a 1:1 CHCl₃/hexanes solvent

Received: July 22, 2023 Revised: October 4, 2023 Published: October 20, 2023





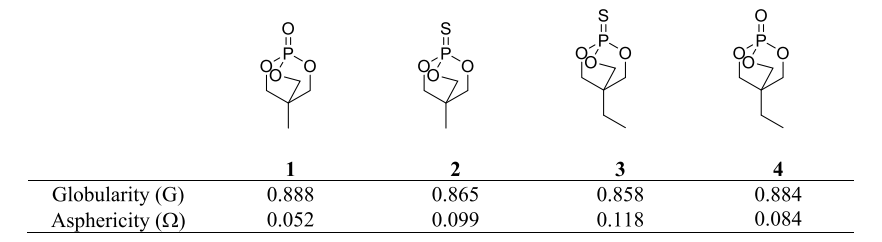


Figure 1. Phosphates studied for their globularity and asphericity.

mixture, and 4 from acetone. All four compounds are in orthorhombic crystal systems, with 1-3 being needle morphology and 4 being block morphology. The crystals of 4 are brittle, meaning elastic and plastic bending are not possible; thus, 4 is not discussed further. The major intermolecular interactions in 1 and 2 are C-H···O hydrogen bonds, whereas for 3, there are C-H···S and C-H···O hydrogen bonds as well as S···O interactions (Figure S2). In the crystal structures, molecules of 1 and 2 are aligned in a head-to-tail arrangement (head = P=O or P=S, δ ⁻; tail = methyl, δ ⁺) along the c-axis in a slanted fashion (Figure 2). The

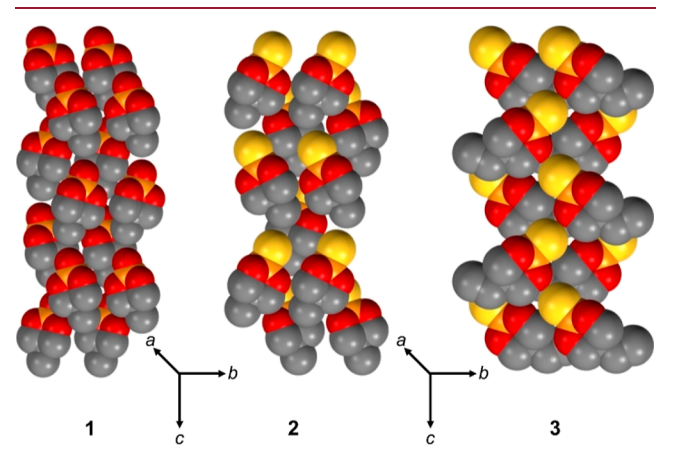


Figure 2. Space-filling model depicting the linear molecular packing in 1 and 2 along the c-axis and depiction of orthogonal packing along the a-axis in 3.

head-to-tail arrangement in 1 $[d_{O\cdots C} = 3.404(5) \text{ Å, } \angle P = O\cdots C = 165.0(2)^{\circ}]$ is more linear comparison to 2 $[d_{S\cdots C} = 3.505(6) \text{ Å, } \angle P = S\cdots C = 140.99(11)^{\circ}]$. However, in 3, the head and tail regions are arranged along the *c*-axis in a corrugated manner with two adjacent molecules interacting via a weak S···O interaction $[d_{S\cdots O} = 3.255(5) \text{ Å, } \angle P = S\cdots O = 171.92(11)^{\circ}]$ (Figure S3).

PLASTIC BENDING

The major faces in the three crystals correspond to the $(\overline{110})$, $(\overline{1}10)$, and (001) planes that were obtained by face indexing. Upon applying mechanical stress along the (001) and $(00\overline{1})$ faces at 23 °C, the crystal bends on the $(\overline{110})$ and $(\overline{110})$ faces into a hairpin shape that could be mechanically straightened but not to its original pristine condition (Figure 3a,b). Uniaxial stress orthogonal to the $(\overline{110})$ face of 1 at 23 °C results in crystals of 1 being pressed into thin sheets. An X-ray diffraction image of the thin sheet $(23\ ^{\circ}\text{C})$, cold pressing) indicates that the crystal is losing its crystalline integrity, whereas the image at $150\ ^{\circ}\text{C}$ (hot pressing) reveals that it has become polycrystalline. Crystals of 1 can also be deformed into other shapes, specifically coils and boxes (Figure S5). The malleable nature of 1 validates our hypothesis that globular bicyclic phosphates can possess mechanical properties.

To understand the plastic bending in the crystals of 1, the arrangement of the molecules in the crystal lattice was analyzed. As depicted in Figure 2, molecules of 1 are stacked along the c-axis in a head-to-tail arrangement to form molecular columns. Around the columns, multiple slip planes exist (Figure 3c). The columns are interconnected by weak

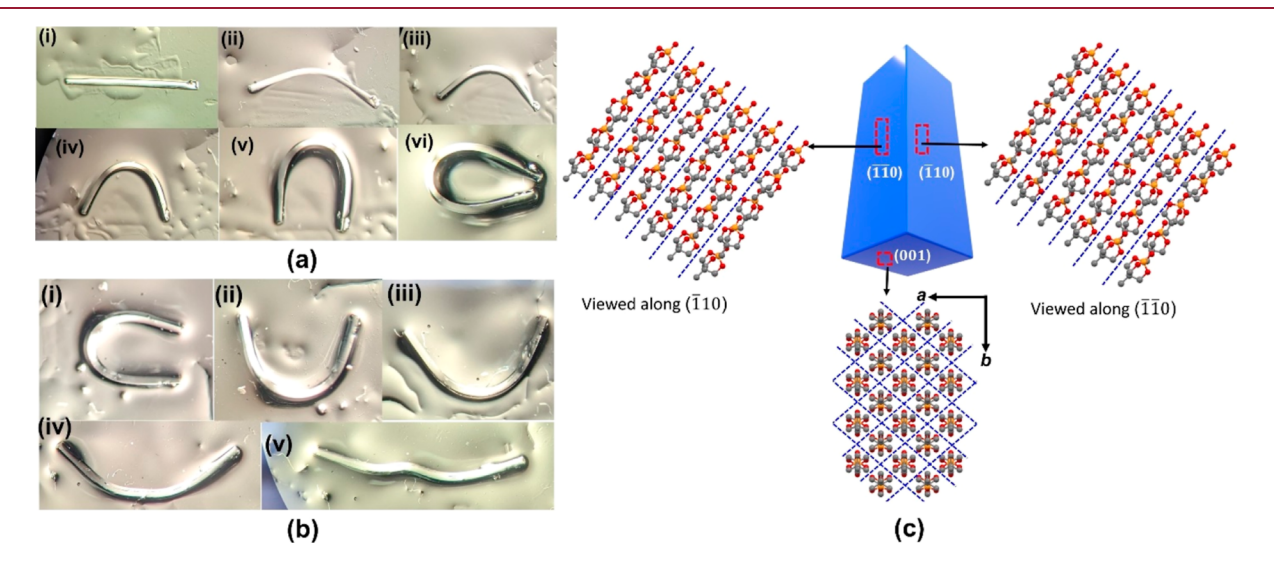


Figure 3. (a) (i) Pristine state; (ii—vi) plastic deformation of 1; (b) mechanical straightening of bent crystals but not to their original pristine condition; (c) molecular packing along different faces and face indexing measurement (dashed blue lines indicate slip planes).

dispersive C-H···O interactions, forming a 2D molecular sheet parallel to the $(\overline{110})$ plane. Upon viewing down the $(\overline{110})$ and $(\overline{110})$ directions, the slip planes between the molecular sheets are apparent. Thus, upon applying stress along the (001) direction, 1 undergoes plastic deformation along these planes.

Plastic bending is also observed in crystals of 2, confirmed by applying stress along the (001) direction, with the bending face corresponding to the (010) plane. Crystals of 2 are flexible in bending but cannot be restored to their original morphology. The head-to-tail packing arrangement along the (001) direction of the molecules in the crystal structures of 1 and 2 are similar but more slanted in 2, resulting in more isotropic packing. The slanted slip planes along the (010) direction in 2 are less favorable for plastic bending, further corroborated by calculations vide infra. In 3, there is no plastic bending, attributed to the orthogonal molecular arrangement that does not have any slip planes.

ELASTIC BENDING

Given the absence of plastic bending in 3, three-point bending experiments were performed on single crystals to determine if elastic bending is possible. Forceps were used to restrain the ends of the single crystal and force was applied to the center with a needle (Figure 4). Gratifyingly, elastic bending was

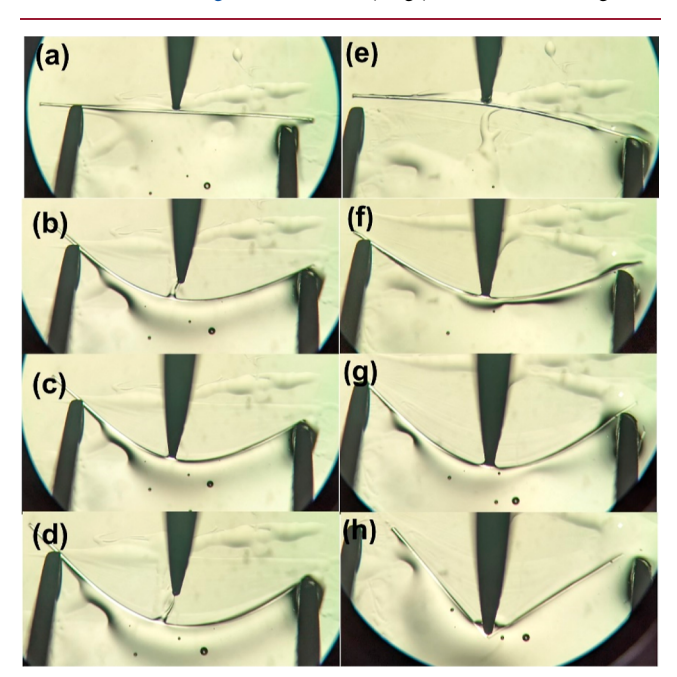


Figure 4. Mechanical properties of single crystals of 3. (a-c) Applying mild force; (d,e) release of the force; and (f-h) applying strong force to fracture the crystal.

possible by applying stress on the (010) plane to bend crystals of 3, and releasing the force resulted in the crystal regaining its original state without fracture (Figure 4e). The elastic bending experiment was repeated three times to confirm the reversibility (Figure 4f,g). However, applying a stronger force fractures the crystal (Figure 4g,h).

Elastic bending requires an expansion of the macroscopic dimension that becomes the outer arc and contraction of the dimension that becomes the inner arc. At the molecular level, the intermolecular interactions also undergo expansion and contraction to accommodate this stress.

To understand the elastic bending of 3, we investigated the molecular packing arrangement along the (100), (010), and (001) faces (Figure S11a). The molecules are stacked along the c-axis in a slanted fashion to form a column. The columns are interconnected by weak P=S···O [d = 3.255(5) Å, $\theta =$ $171.92(11)^{\circ}$] interactions to form corrugated sheets on the *bc*plane (Figure 5a). This S···O interaction acts as a structural buffer, where the geometry of interacting molecules of adjacent columns is orthogonal to each other. The electron-rich oxygen interacts with the electron-deficient zone of sulfur, as shown by its electrostatic potential maps clearly indicating the S···O interaction is a σ -hole interaction (ESP, Figures 5b and S24c). 25,51 Applying stress along the (010) direction, the S···O structural buffers can undergo expansion (outer arc) or contraction (inner arc) leading to the elastic behavior depicted in Figure 5c. The molecular arrangement in the (100) and (001) directions also exhibits isotropy in the internal structure.

■ ENERGY FRAMEWORK CALCULATIONS

To understand the mechanical behavior, the pairwise interaction energies were calculated based on the energy frameworks using CrystalExplorer. 52-54 Framework calculations provide insights into the anisotropic interactions to correlate their bending effects in mechanosalient crystals. 55,56 In 1, the total energy frameworks viewed along the $(\overline{110})$ plane reveal destabilizing frameworks between the molecular sheets that facilitate slippage upon applying stress (Figure S13). To quantify the energetics of slips, frameworks can be segregated into three components: columns, sheets, and slips. The molecules propagating along the (001) direction form 1D columns with a net interaction energy of -38.6 kJ/mol, and the major contribution is from the attractive electrostatic component (-27.6 kJ/mol). These columns interact with adjacent columns to form molecular sheets with a net interaction energy of -117.3 kJ/mol (Figures S14b and S15b). The corresponding slips between the molecular sheets have a net slip plane energy of -42.8 kJ/mol. The slip plane is composed of strong destabilizing Coulombic interactions. This quantitatively depicts the energetic anisotropy in the intermolecular interactions in the crystal lattice that leads to low-energy slip planes along the $(\overline{110})$ direction. Similar destabilizing frameworks exist between the slips down the (010) direction in 2. The energies of the molecular sheet and the slip plane along (010) are considerably higher in 2 than those in 1, at -65.5 and -86.0 kJ/mol, respectively. This supports the experimental observation that 2 has less plastic behavior than 1 as the slip energies are much higher.

Quantifying the structural isotropy of 3 by energy frameworks reveals that the frameworks down the (010) direction clearly depict an isotropic interaction pattern within the crystal lattice of 3 (Figure 6). Based on the energy frameworks, the molecular columns stacked along the (001) direction (Figure 5a) are strongly dispersive with a total interaction energy of -27.0 kJ/mol. The dispersion forces are the major contributor (-13.2 kJ/mol), with the interaction energy between the columns being lower (-6.6 kJ/mol represented in Figure 5a as the structural buffer region).

COMPUTATIONAL ANALYSIS

The frontier molecular orbitals (HOMO and LUMO) and electrostatic potential (ESP) maps were computed.⁵⁷ In 1, the HOMO is distributed around the bicyclic ring system and the

Crystal Growth & Design pubs.acs.org/crystal Article

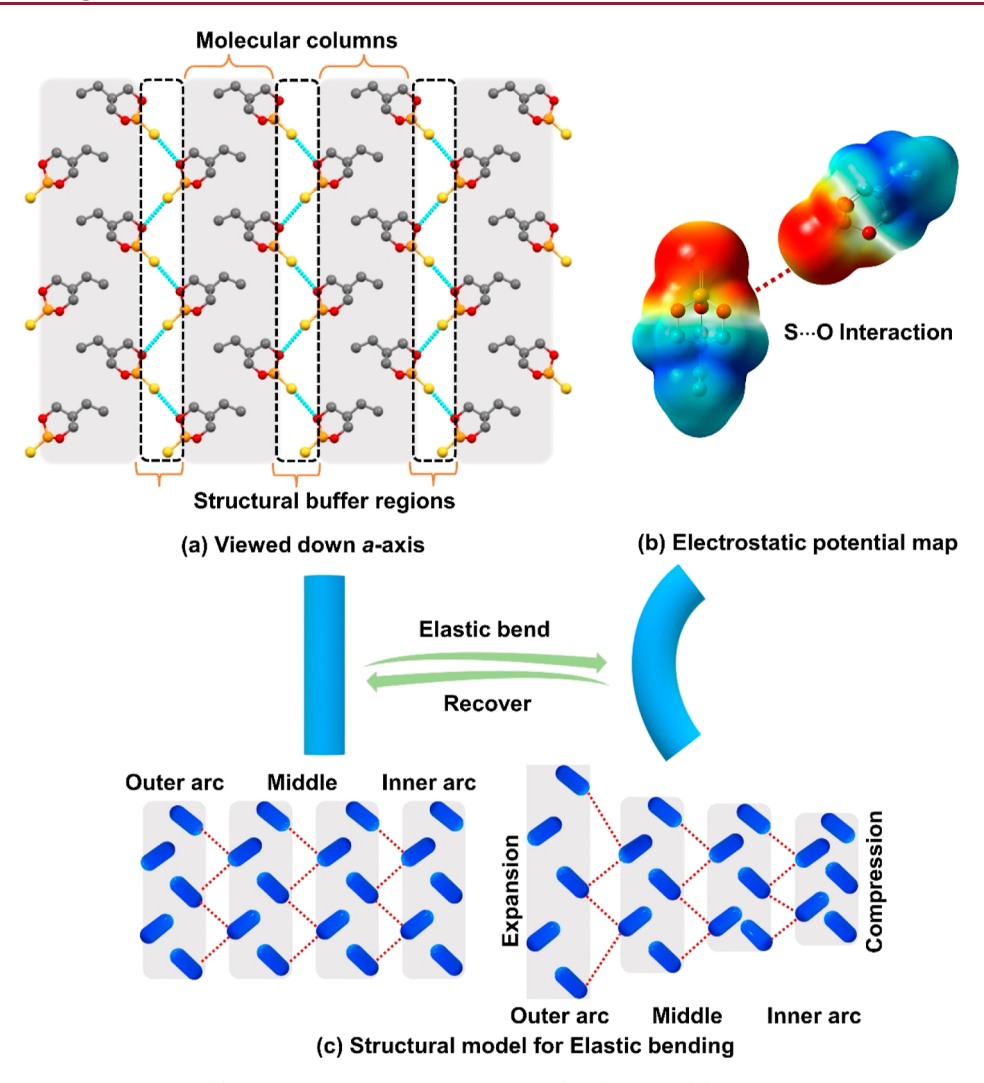


Figure 5. Bending mechanism analyses, (a) crystal packing viewed along the (100) plane; (b) electrostatic potential map of 3; (c) schematic illustrating elastic bending at the molecular level.

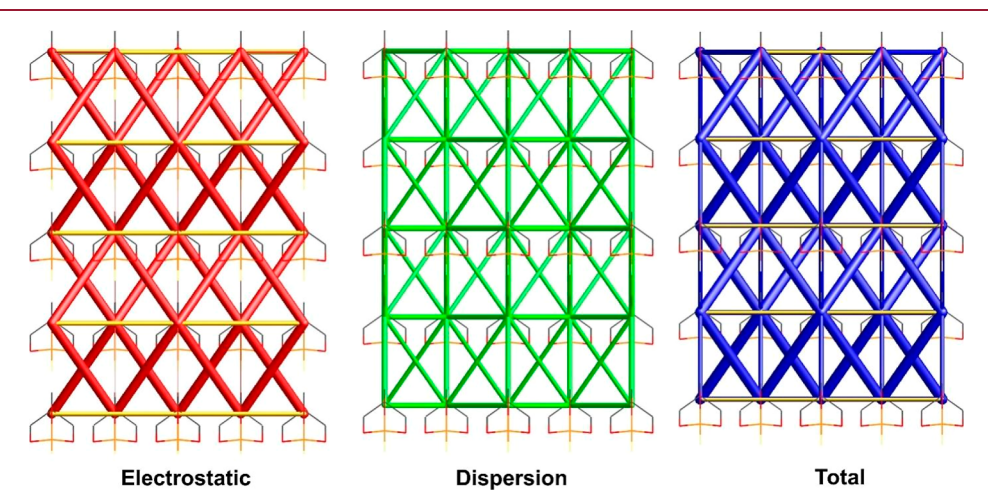


Figure 6. Energy frameworks for 3 viewed down the (010); electrostatic (red), dispersion (green), and total interaction energy (blue).

LUMO around the $-CH_3$ group. In 2, the LUMO is in the same position as 1 but the HOMO is centered around the sulfur atom. The ESPs show a high polarizability for 1–3. The energy frameworks and the ESP profile both indicate strong electrostatic molecular interactions along the c-axis. ⁵² The magnitude of the interaction energy in 1 is higher than that in

2 because adjacent molecules are packed closer and arranged in a more linear fashion. The strong destabilizing interaction in 1, as observed in the energy frameworks, correlates with the orbital profile and the ESP map. This is accounted for by the repulsion of the electron-rich regions of adjacent molecules in the column. The repulsion is more prominent in 1 compared

Crystal Growth & Design pubs.acs.org/crystal Article

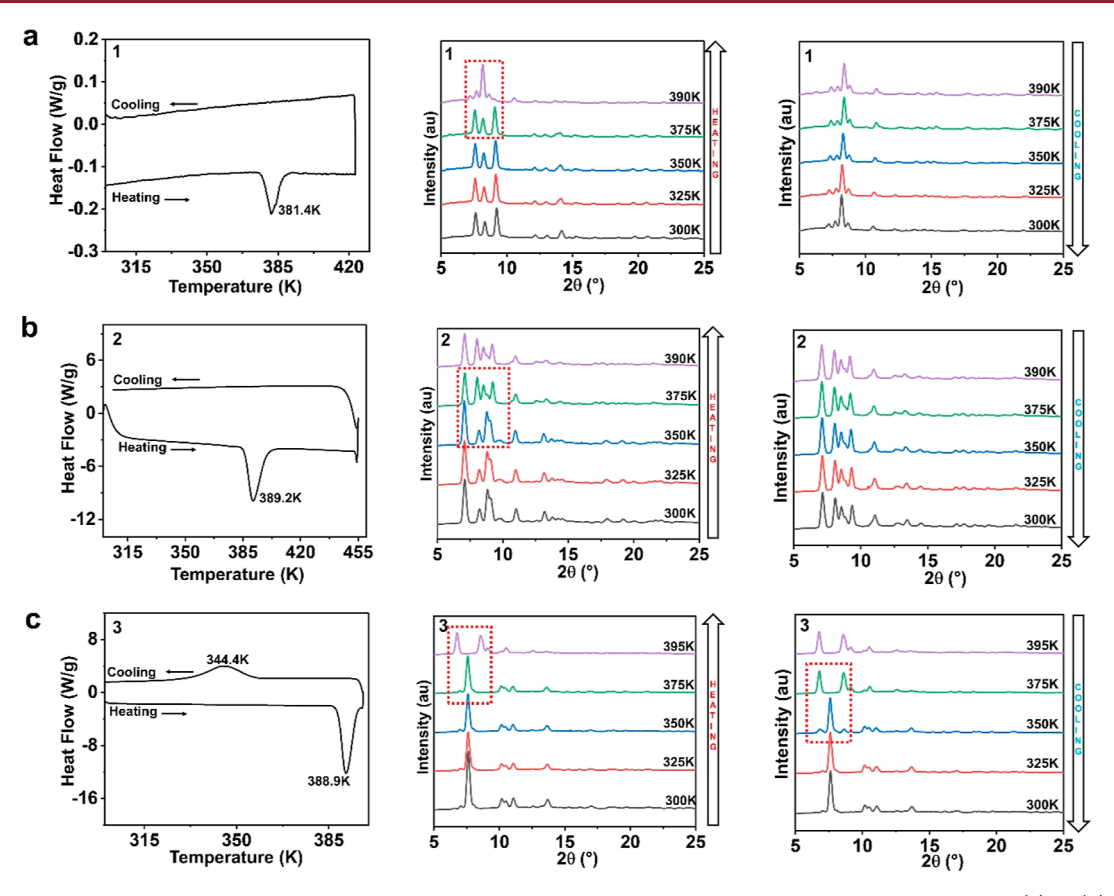


Figure 7. DSC traces and corresponding variable temperature powder X-ray diffraction pattern upon heating and cooling of (a) 1, (b) 2, and (c) 3.

to 2 rationalized by the greater magnitude of the negative surface in the ESP maps.

■ PHASE TRANSITION STUDIES

Differential scanning calorimetry (DSC) experiments were performed to understand the phase transition behaviors of 1-3. All three showed a phase transformation upon heating with endothermic peaks at 381.4, 389.2, and 388.9 K for 1-3, respectively (Figure 7). The transition observed is irreversible in 1 and 2 with no exothermic peak during the cooling cycle. However, the transition in 3 is reversible with a broad exothermic peak at 344.7 K and a thermal hysteresis of 45.5 K (Figure 7c). The presence of a wide thermal hysteresis indicates first-order phase transition behavior. The entropic changes (ΔS) during the heating and cooling cycles were calculated based on the enthalpy of transition (ΔH) for 1–3. The entropy changes (ΔS) for the heating cycles were computed to be 5.13, 7.71, and 16.14 J mol^{-1} K⁻¹ for 1-3, respectively. The entropy change (ΔS) for the cooling cycle of 3 is $11.86 \text{ J mol}^{-1} \text{ K}^{-1}$. The ratios of the number of high to low geometrically distinguishable orientations (N) were computed from the Boltzmann equation ($\Delta S = R \ln N$, R = ideal gas constant or 8.314 J mol^{-1} K⁻¹). The N values for the heating cycles are 1.85, 5.13, and 6.97 for 1-3, respectively, while the cooling cycle of 3 is 4.17. A value of N greater than unity indicates a high degree of disorder in the structure above the transition temperature confirming that an order-disorder structural transition is occurring. \$8-62 To confirm that the phase transition is not a decomposition, TGA experiments were carried out from 300 to 750 K. Compounds 1-3 are

stable up to 440 K, far beyond their transition temperatures (Figure S26).

Thermal experiments were validated using variable temperature powder X-ray diffraction experiments. Initial phase purity was confirmed by comparing the experimental pattern at 300 K to the simulated patterns. During the heating process at a ramp rate of 4 K min⁻¹, structural phase transformations in 1–3 at similar temperature ranges to DSC transition temperatures (highlighted in red zones in Figure 7). After cooling, the diffraction pattern of the high-temperature phase remains constant after dropping from 395 to 300 K in 1 and 2, confirming the irreversible nature of the phase transition. Contrarily, in 3, the diffraction pattern reverts to the original state indicating reversibility (Figure 7).

Interestingly, as mentioned above in the DSC experiment of 1, after heating and a subsequent cooling cycle, there was not a transition as validated by powder X-ray diffraction. However, storing the sample overnight and obtaining the powder X-ray diffraction pattern indicates that it reverts to the original state revealing reversibility but the process is sluggish compared to 3 (Figure S28). To confirm the reversibility, the temperature ramp rate was decreased from 4 to 0.5 K min⁻¹ and cooled at the same rate for a fresh sample. The heating cycle reveals a phase transformation in the same temperature window, but during the cooling cycle, the transition back to the initial state is at approximately 320 K, lower than the heating transition (Figure S29). This indicates that the reversible phase transformation of 1 is slow.

CONCLUSIONS

In this work, plastic and elastic bending in globular bicyclic phosphate oxides and sulfides featuring methyl and ethyl tails is described. Three of the four compounds exhibit bending properties, with two being plastic bending and one featuring elastic bending. The plastic single crystals can be molded into different shapes. The structure—property relationship is analyzed by the single-crystal X-ray diffraction data and energy framework calculations. All three of these globular systems undergo temperature-induced phase transitions, with the transitions in 1 and 3 being reversible and 2 irreversible. The polar crystallographic space group, high dipole moment, and large charge separation based on their ESP maps fulfill the required criteria to be explored as potential ferroelectric materials with high mechanical flexibility.

ASSOCIATED CONTENT

Solution Supporting Information

The Supporting Information is available free of charge at https://pubs.acs.org/doi/10.1021/acs.cgd.3c00866.

Crystallographic details, computational details, powder X-ray diffraction, and additional figures (PDF)

Movie of bending in 3 (MP4)

Accession Codes

CCDC 2279268–2279273, 2298594, and 2298708 contain the supplementary crystallographic data for this paper. These data can be obtained free of charge via www.ccdc.cam.ac.uk/data_request/cif, or by emailing data_request@ccdc.cam.ac.uk, or by contacting the Cambridge Crystallographic Data Centre, 12 Union Road, Cambridge CB2 1EZ, UK; fax: +44 1223 336033.

AUTHOR INFORMATION

Corresponding Author

Caleb D. Martin — Department of Chemistry and Biochemistry, Baylor University, Waco, Texas 76798, United States; Occid.org/0000-0001-9681-0160; Email: caleb d martin@baylor.edu

Author

Sanjay Dutta – Department of Chemistry and Biochemistry, Baylor University, Waco, Texas 76798, United States

Complete contact information is available at: https://pubs.acs.org/10.1021/acs.cgd.3c00866

Author Contributions

The manuscript was written through contributions of all authors. All authors have given approval to the final version of the manuscript.

Notes

The authors declare no competing financial interest.

ACKNOWLEDGMENTS

We are grateful to Baylor University, the Welch Foundation (grant no. AA-1846), and the National Science Foundation (award no. 1753025) for their generous support of this work. We thank Blake Haller and Nathan Emerson from the Baylor Research and Innovation Collaborative (BRIC) for assisting with differential scanning calorimetry and thermogravimetric analysis.

REFERENCES

- (1) Lipomi, D. J.; Tee, B. C. K.; Vosgueritchian, M.; Bao, Z. Stretchable organic solar cells. *Adv. Mater.* **2011**, 23 (15), 1771–1775.
- (2) Naumov, P.; Chizhik, S.; Panda, M. K.; Nath, N. K.; Boldyreva, E. Mechanically responsive molecular crystals. *Chem. Rev.* **2015**, *115* (22), 12440–12490.
- (3) Saha, S.; Mishra, M. K.; Reddy, C. M.; Desiraju, G. R. From molecules to interactions to crystal engineering: mechanical properties of organic solids. *Acc. Chem. Res.* **2018**, *51* (11), 2957–2967.
- (4) Thompson, A. J.; Chamorro Orué, A. I.; Nair, A. J.; Price, J. R.; McMurtrie, J.; Clegg, J. K. Elastically flexible molecular crystals. *Chem. Soc. Rev.* **2021**, *50* (21), 11725–11740.
- (5) Awad, W. M.; Davies, D. W.; Kitagawa, D.; Mahmoud Halabi, J.; Al-Handawi, M. B.; Tahir, I.; Tong, F.; Campillo-Alvarado, G.; Shtukenberg, A. G.; Alkhidir, T.; et al. Mechanical properties and peculiarities of molecular crystals. *Chem. Soc. Rev.* **2023**, 52 (9), 3098–3169.
- (6) Chizhik, S.; Sidelnikov, A.; Zakharov, B.; Naumov, P.; Boldyreva, E. Quantification of photoinduced bending of dynamic molecular crystals: from macroscopic strain to kinetic constants and activation energies. *Chem. Sci.* **2018**, *9* (8), 2319–2335.
- (7) Mahmoud Halabi, J.; Ahmed, E.; Sofela, S.; Naumov, P. Performance of molecular crystals in conversion of light to mechanical work. *Proc. Natl. Acad. Sci. U.S.A.* **2021**, *118* (5), No. e2020604118.
- (8) Fratzl, P.; Barth, F. G. Biomaterial systems for mechanosensing and actuation. *Nature* **2009**, *462* (7272), 442–448.
- (9) Stoddart, J. F. Mechanically interlocked molecules (MIMs)-molecular shuttles, switches, and machines (Nobel Lecture). *Angew. Chem., Int. Ed.* **2017**, *56* (37), 11094–11125.
- (10) Dattler, D.; Fuks, G.; Heiser, J.; Moulin, E.; Perrot, A.; Yao, X.; Giuseppone, N. Design of collective motions from synthetic molecular switches, rotors, and motors. *Chem. Rev.* **2020**, *120* (1), 310–433.
- (11) Hayashi, S.; Koizumi, T. Mechanically induced shaping of organic single crystals: Facile fabrication of fluorescent and elastic crystal fibers. *Chem.—Eur. J.* **2018**, *24* (34), 8507–8512.
- (12) Hayashi, S.; Koizumi, T. Elastic Organic Crystals of a Fluorescent π -Conjugated Molecule. *Angew. Chem., Int. Ed.* **2016**, 55 (8), 2701–2704.
- (13) Hayashi, S.; Asano, A.; Kamiya, N.; Yokomori, Y.; Maeda, T.; Koizumi, T. Fluorescent organic single crystals with elastic bending flexibility: 1,4-bis(thien-2-yl)-2,3,5,6-tetrafluorobenzene derivatives. *Sci. Rep.* **2017**, *7* (1), 9453.
- (14) Naim, K.; Singh, M.; Sharma, S.; Nair, R. V.; Venugopalan, P.; Chandra Sahoo, S.; Neelakandan, P. P. Exceptionally Plastic/Elastic Organic Crystals of a Naphthalidenimine Boron Complex Show Flexible Optical Waveguide Properties. *Chem.—Eur. J.* **2020**, *26* (52), 11979–11984.
- (15) Liu, T.; Li, Y.; Yan, Y.; Li, Y.; Yu, Y.; Chen, N.; Chen, S.; Liu, C.; Zhao, Y.; Liu, H. Tuning Growth of Low-Dimensional Organic Nanostructures for Efficient Optical Waveguide Applications. *J. Phys. Chem. C* 2012, *116* (26), 14134–14138.
- (16) Zhang, C.; Zhao, Y. S.; Yao, J. Optical waveguides at micro/nanoscale based on functional small organic molecules. *Phys. Chem. Chem. Phys.* **2011**, *13* (20), 9060–9073.
- (17) Annadhasan, M.; Agrawal, A. R.; Bhunia, S.; Pradeep, V. V.; Zade, S. S.; Reddy, C. M.; Chandrasekar, R. Mechanophotonics: Flexible Single-Crystal Organic Waveguides and Circuits. *Angew. Chem., Int. Ed.* **2020**, *59* (33), 13852–13858.
- (18) Huang, R.; Wang, C.; Wang, Y.; Zhang, H. Elastic Self-Doping Organic Single Crystals Exhibiting Flexible Optical Waveguide and Amplified Spontaneous Emission. *Adv. Mater.* **2018**, *30* (21), 1800814.
- (19) Lan, L.; Yang, X.; Tang, B.; Yu, X.; Liu, X.; Li, L.; Naumov, P.; Zhang, H. Hybrid elastic organic crystals that respond to aerial humidity. *Angew. Chem., Int. Ed.* **2022**, *61* (14), No. e202200196.
- (20) Rupasinghe, T. P.; Hutchins, K. M.; Bandaranayake, B. S.; Ghorai, S.; Karunatilake, C.; Bučar, D. K.; Swenson, D. C.; Arnold, M. A.; MacGillivray, L. R.; Tivanski, A. V. Mechanical Properties of a

- Series of Macro- and Nanodimensional Organic Cocrystals Correlate with Atomic Polarizability. *J. Am. Chem. Soc.* **2015**, *137* (40), 12768–12771
- (21) Ghosh, S.; Reddy, C. M. Elastic and Bendable Caffeine Cocrystals: Implications for the Design of Flexible Organic Materials. *Angew. Chem., Int. Ed.* **2012**, *51* (41), 10319–10323.
- (22) Ghosh, S.; Mishra, M. K.; Kadambi, S. B.; Ramamurty, U.; Desiraju, G. R. Designing elastic organic crystals: highly flexible polyhalogenated n benzylideneanilines. *Angew. Chem., Int. Ed.* **2015**, 54 (9), 2674–2678.
- (23) Hayashi, S.; Koizumi, T.; Kamiya, N. Elastic bending flexibility of a fluorescent organic single crystal: New aspects of the commonly used building block 4, 7-dibromo-2, 1, 3-benzothiadiazole. *Cryst. Growth Des.* **2017**, *17* (12), 6158–6162.
- (24) Mishra, M. K.; Mishra, K.; Syed Asif, S. A.; Manimunda, P. Structural analysis of elastically bent organic crystals using in situ indentation and micro-Raman spectroscopy. *Chem. Commun.* **2017**, 53 (97), 13035–13038.
- (25) Saha, S.; Desiraju, G. R. σ -Hole and π -Hole Synthon Mimicry in Third-Generation Crystal Engineering: Design of Elastic Crystals. *Chem.—Eur. J.* **2017**, 23 (20), 4936–4943.
- (26) Thomas, S. P.; Shi, M. W.; Koutsantonis, G. A.; Jayatilaka, D.; Edwards, A. J.; Spackman, M. A. The elusive structural origin of plastic bending in dimethyl sulfone crystals with quasi isotropic crystal packing. *Angew. Chem., Int. Ed.* **2017**, *56* (29), 8468–8472.
- (27) Worthy, A.; Grosjean, A.; Pfrunder, M. C.; Xu, Y.; Yan, C.; Edwards, G.; Clegg, J. K.; McMurtrie, J. C. Atomic resolution of structural changes in elastic crystals of copper (II) acetylacetonate. *Nat. Chem.* **2018**, *10* (1), 65–69.
- (28) Abeysekera, A. M.; Averkiev, B. B.; Sinha, A. S.; Aakeröy, C. B. Evaluating structure-property relationship in a new family of mechanically flexible co-crystals. *Chem. Commun.* **2022**, *58* (68), 9480–9483.
- (29) Bhandary, S.; Thompson, A. J.; McMurtrie, J. C.; Clegg, J. K.; Ghosh, P.; Mangalampalli, S. R. N. K.; Takamizawa, S.; Chopra, D. The mechanism of bending in a plastically flexible crystal. *Chem. Commun.* **2020**, *56* (84), 12841–12844.
- (30) Manoharan, D.; Ahmad, S.; Emmerling, F.; Bhattacharya, B.; Ghosh, S. Stress and light sensitive dual-mechanical property of acylhydrazone crystal. *CrystEngComm* **2023**, *25* (21), 3237–3244.
- (31) Mišura, O.; Pisačić, M.; Borovina, M.; Daković, M. Tailoring Enhanced Elasticity of Crystalline Coordination Polymers. *Cryst. Growth Des.* **2023**, 23 (3), 1318–1322.
- (32) Wang, K.; Mishra, M. K.; Sun, C. C. Exceptionally Elastic Single-Component Pharmaceutical Crystals. *Chem. Mater.* **2019**, *31* (5), 1794–1799.
- (33) Zhu, L.; Al-Kaysi, R. O.; Bardeen, C. J. Reversible photo-induced twisting of molecular crystal microribbons. *J. Am. Chem. Soc.* **2011**, 133 (32), 12569–12575.
- (34) Cui, X.; Rohl, A. L.; Shtukenberg, A.; Kahr, B. Twisted aspirin crystals. *J. Am. Chem. Soc.* **2013**, *135* (9), 3395–3398.
- (35) Saha, S.; Desiraju, G. R. Crystal engineering of hand-twisted helical crystals. J. Am. Chem. Soc. 2017, 139 (5), 1975–1983.
- (36) Chen, K.; Wang, J.; Feng, Y.; Liu, H.; Zhang, X.; Hao, Y.; Wang, T.; Huang, X.; Hao, H. Multiple stimuli-responsive flexible crystal with 2D elastic bending, plastic twisting and photoinduced bending capabilities. *J. Mater. Chem. C* **2021**, *9* (46), 16762–16770.
- (37) Saha, S.; Desiraju, G. R. A hand-twisted helical crystal based solely on hydrogen bonding. *Chem. Commun.* **2017**, *53* (47), 6371–6374.
- (38) Kim, T.; Zhu, L.; Mueller, L. J.; Bardeen, C. J. Mechanism of Photoinduced Bending and Twisting in Crystalline Microneedles and Microribbons Composed of 9-Methylanthracene. *J. Am. Chem. Soc.* **2014**, *136* (18), 6617–6625.
- (39) Gupta, P.; Karothu, D. P.; Ahmed, E.; Naumov, P.; Nath, N. K. Thermally Twistable, Photobendable, Elastically Deformable, and Self-Healable Soft Crystals. *Angew. Chem., Int. Ed.* **2018**, *57* (28), 8498–8502.

- (40) Mondal, A.; Bhattacharya, B.; Das, S.; Bhunia, S.; Chowdhury, R.; Dey, S.; Reddy, C. M. Metal like Ductility in Organic Plastic Crystals: Role of Molecular Shape and Dihydrogen Bonding Interactions in Aminoboranes. *Angew. Chem., Int. Ed.* **2020**, 59 (27), 10971–10980.
- (41) Kim, T.; Al-Muhanna, M. K.; Al-Suwaidan, S. D.; Al-Kaysi, R. O.; Bardeen, C. J. Photoinduced Curling of Organic Molecular Crystal Nanowires. *Angew. Chem., Int. Ed.* **2013**, 52 (27), 6889–6893.
- (42) Xie, P.; Zhang, R. Liquid crystal elastomers, networks and gels: advanced smart materials. J. Mater. Chem. 2005, 15 (26), 2529–2550.
- (43) Ikeda, T.; Mamiya, J.-i.; Yu, Y. Photomechanics of Liquid-Crystalline Elastomers and Other Polymers. *Angew. Chem., Int. Ed.* **2007**, 46 (4), 506–528.
- (44) Pelrine, R.; Kornbluh, R.; Pei, Q.; Joseph, J. High-Speed Electrically Actuated Elastomers with Strain Greater Than 100%. *Science* **2000**, 287 (5454), 836–839.
- (45) Ghosh, S.; Mishra, M. K. Elastic Molecular Crystals: From Serendipity to Design to Applications. *Cryst. Growth Des.* **2021**, *21* (4), 2566–2580.
- (46) Reddy, C. M.; Padmanabhan, K. A.; Desiraju, G. R. Structure-Property Correlations in Bending and Brittle Organic Crystals. *Cryst. Growth Des.* **2006**, *6* (12), 2720–2731.
- (47) Das, S.; Saha, S.; Sahu, M.; Mondal, A.; Reddy, C. M. Temperature reliant dynamic properties and elasto plastic to plastic crystal (rotator) phase transition in a metal oxyacid salt. *Angew. Chem., Int. Ed.* **2022**, *61* (8), No. e202115359.
- (48) Silva, J. F. C.; Rosado, M. T. S.; Jasiurkowska-Delaporte, M.; Silva, M. R.; Piedade, M. F. M.; Dryzek, E.; Eusébio, M. E. S. Ordered and Plastic Crystals in the Complex Polymorphism of Pinanediol. *Cryst. Growth Des.* **2019**, *19* (11), 6127–6135.
- (49) Xing, W.; Song, L.; Lu, H.; Hu, Y.; Zhou, S. Flame retardancy and thermal degradation of intumescent flame retardant polypropylene with MP/TPMP. *Polym. Adv. Technol.* **2009**, *20* (8), 696–702.
- (50) Zhang, G.; Song, D.; Ma, S.; Wang, Y.; Xie, X.; Dong, Y. A novel P-S-Si-based cage-structural monomer for flame-retardant modification of unsaturated polyester resin. *Polym. Adv. Technol.* **2021**, 32 (4), 1604–1614.
- (51) Moaven, S.; Yu, J.; Vega, M.; Unruh, D. K.; Cozzolino, A. F. Self-assembled reversed bilayers directed by pnictogen bonding to form vesicles in solution. *Chem. Commun.* **2018**, *54* (64), 8849–8852.
- (52) Turner, M. J.; Thomas, S. P.; Shi, M. W.; Jayatilaka, D.; Spackman, M. A. Energy frameworks: insights into interaction anisotropy and the mechanical properties of molecular crystals. *Chem. Commun.* **2015**, *51* (18), 3735–3738.
- (53) Mackenzie, C. F.; Spackman, P. R.; Jayatilaka, D.; Spackman, M. A. CrystalExplorer model energies and energy frameworks: extension to metal coordination compounds, organic salts, solvates and open-shell systems. *IUCrJ* **2017**, *4* (5), 575–587.
- (54) Wolff, S.; Grimwood, D.; McKinnon, J.; Turner, M.; Jayatilaka, D.; Spackman, M. *Crystal Explorer*; University of Western Australia Crawley: Australia, 2012.
- (55) Wang, C.; Sun, C. C. Identifying Slip Planes in Organic Polymorphs by Combined Energy Framework Calculations and Topology Analysis. *Cryst. Growth Des.* **2018**, *18* (3), 1909–1916.
- (56) Raju, K. B.; Ranjan, S.; Vishnu, V. S.; Bhattacharya, M.; Bhattacharya, B.; Mukhopadhyay, A. K.; Reddy, C. M. Rationalizing Distinct Mechanical Properties of Three Polymorphs of a Drug Adduct by Nanoindentation and Energy Frameworks Analysis: Role of Slip Layer Topology and Weak Interactions. *Cryst. Growth Des.* **2018**, *18* (7), 3927–3937.
- (57) Gaussian 16, Rev. C.01: Wallingford, CT, 2016.
- (58) Chen, S.-P.; Wang, C.-F.; Zhou, H.-T.; Tan, Y.-H.; Wen, H.-R.; Tang, Y.-Z. Ferroelectric Property, Switchable Dielectric, and Excellent Second Harmonic Generation Response in a Homochiral Organic Salt: l-Prolinammonium 1-Adamantane Carboxylate. *Cryst. Growth Des.* **2018**, *18* (10), 6117–6122.
- (59) Tang, Y.-Z.; Yu, Y.-M.; Xiong, J.-B.; Tan, Y.-H.; Wen, H.-R. Unusual High-Temperature Reversible Phase-Transition Behavior, Structures, and Dielectric-Ferroelectric Properties of Two New

- Crown Ether Clathrates. J. Am. Chem. Soc. 2015, 137 (41), 13345-13351.
- (60) Chen, X.-G.; Zhang, Y.-Z.; Sun, D.-S.; Gao, J.-X.; Hua, X.-N.; Liao, W.-Q. Above room-temperature dielectric and nonlinear optical switching materials based on $[(CH_3)_3S]_2[MBr_4]$ (M = Cd, Mn and Zn). Dalton Trans. 2019, 48 (30), 11292–11297.
- (61) Li, L.-S.; Tan, Y.-H.; Wei, W.-J.; Gao, H.-Q.; Tang, Y.-Z.; Han, X.-B. Chiral Switchable Low-Dimensional Perovskite Ferroelectrics. *ACS Appl. Mater. Interfaces* **2021**, *13* (1), 2044–2051.
- (62) Panicker, L.; Thomas, S. P.; Wadawale, A.; Girija, K. G.; Row, T. G. Reversible order-disorder phase transition and interaction topology in 4-carboxyanilinium nitrate. *J. Mol. Struct.* **2021**, 1227, 129542.